Modeling the reflection from cholesteric liquid crystals using modal analysis and mode matching

Marios Andreas Christou,* Nectarios C. Papanicolaou,† and Anastasis C. Polycarpou‡
University of Nicosia, 46 Makedonitissas Avenue, P.O. Box 24005, 1700 Nicosia, Cyprus
(Received 5 December 2011; published 9 March 2012)

The reflection and transmission spectra from right-handed cholesteric liquid crystals are computed in the visible region for a linearly, circularly, or elliptically polarized incident plane wave at oblique incidence. The liquid crystal cell is sandwiched between dielectric layers of certain thickness and refractive index. The underlined formulation is based on a modal analysis of the governing field expressions in the dielectric and liquid-crystal regions. A representative matrix system is obtained after enforcing the continuity of the tangential electric and magnetic fields at the material interfaces. Solution of the governing matrix system results in the reflectance and transmittance for a given wavelength. Numerical results for both normal and oblique incidence were obtained and compared with data published in the literature. The underlined formulation is effective, accurate, robust, versatile, and computationally efficient.

DOI: 10.1103/PhysRevE.85.031702 PACS number(s): 42.70.Df, 78.20.Bh, 42.25.Bs, 42.25.Lc

I. INTRODUCTION

Cholesteric liquid crystals [1,2] are anisotropic materials where the directors twist along a helical axis which is perpendicular to the director. The helical structure of the director field is periodic and the periodicity is often referred to as the pitch length. As a result, the dielectric tensor entries of a cholesteric liquid crystal are dependent on the coordinate along the axis of the helix. In other words, the material is anisotropic and inhomogeneous. Two methods are often used for the analysis of cholesteric liquid crystals: the Jones matrix method [3] and the Berreman 4×4 matrix method [4,5]. The Jones matrix method is based on subdividing the crystal into thin slices and, using a 2×2 complex matrix operator, the incident polarized field at the lower slice is related to the polarized field emerging from the upper slice. This method is simple and fast; however, it is only applicable to normal incidence and does not take into account multiple reflections within the sublayers. Throughout the years, there were significant contributions to the method in an attempt to improve its accuracy by either taking into account single or multiple reflections from the interfaces or by extending the method to oblique incidence [6–10]. On the other hand, the Berreman method is based on the same technique of slicing the crystal into thin layers and using a 4×4 propagator matrix that relates the tangential electric and magnetic fields at the lower layer interface to the upper layer interface. The Berreman method is more generic than the Jones matrix method as it accounts for multiple reflections inside the layers and is applicable to oblique angles of incidence. An overview and comparison of the two methods can be found in a review paper by Wöhler and Becker [11]. The calculation of the overall propagator matrix, which relates the tangential fields at the entry point to the tangential fields at the exit point, is a computationally intensive process as it results from the matrix multiplication of the individual propagator matrices corresponding to successive layers. In case the thickness of these layers is comparable to the wavelength, each of these layers should be further subdivided thus adding to the computational cost of the algorithm [12]. The layers and sublayers are thin due to the fact that the propagator matrix is calculated based on a Taylor series expansion of an exponential function involving the well-known Berreman matrix. An accurate Taylor expansion requires either small layer thickness or higher-order terms. Alternative faster formulations of the Berreman matrix method have been suggested in an attempt to speed up the computation of the reflectance and transmittance spectra of cholesteric liquid crystals [13–17].

The effect of a dc electric field on electromagnetic wave propagation in cholestericlike materials at oblique incidence was studied extensively by Lakhtakia and co-workers [18–20] using a 4×4 matrix representation and a generalization of the Oseen transformation [21,22]. Exact analytical solutions to the problem of electromagnetic wave propagation in helicoidal structures with definite periodicity have been derived only for the particular case of normal incidence [21,23–25]. For the problem of oblique incidence, truncated series expansions of elliptically polarized plane waves were used by Oldano and co-workers [26–28] to represent forward and backward propagating waves inside the chiral medium. It has been shown that a high degree of accuracy can be reached using a small number of dominant expansion coefficients.

The current formulation is based on the original work by Smith [29,30] and later by Teitler and Henvis [31] on the refraction by stratified anisotropic media. Since the cholesteric liquid crystal is inhomogeneous, thus resulting in a dielectric tensor that is dependent on the coordinate along the helical axis, the crystal cell is subdivided into multiple layers. As in the Berreman matrix method, these layers are considered homogeneous; in other words, the dielectric tensor profile along the helical axis is staircased. Modeling the crystal as a piecewise continuous material was first proposed in 1869 by Reusch [32] and recently expanded upon by Hodgkinson *et al.* [33]. Unlike the Berreman matrix method, in the underlined formulation there is no propagator matrix. Instead, a mode-matching approach is used to enforce the continuity of the tangential field components at the various interfaces, thus

*Department of Mathematics; christou.ma@unic.ac.cy
†Department of Mathematics; papanicolaou.n@unic.ac.cy
‡Department of Electrical and Computer Engineering; polycarpou.a@unic.ac.cy

generating a coefficient matrix that is representative of the problem at hand. The governing matrix system is solved once per wavelength in order to obtain the expansion coefficients of the governing modes inside the liquid crystal and the dielectric layers constituting the cell. In addition, the solution vector provides the corresponding reflection and transmission coefficients based on an obliquely incident plane wave.

The method developed in this paper to solve the problem of electromagnetic wave propagation in cholesteric crystals under oblique incidence is analytical in nature and exact. The only approximation made in our formulation was the staircasing of the helicoidal profile of the dielectric tensor. The error introduced in the solution due to the piecewise continuous nature of the dielectric tensor is exponentially reduced as the number of layers is increased. Thus the underlined formulation is highly accurate and suitable even for the characterization of the higher-order reflection bands of cholesterics, which are known to exist only for light at oblique incidence [28,34,35].

In the following section, we present the mathematical formulation starting from the Maxwell equations, in order to obtain the governing field expressions inside the dielectrics and chiral medium, and continue to derive the linear set of equations after enforcing the continuity of the tangential fields at the interfaces. In Sec. III, we present numerical results on the reflectance and transmittance at normal and oblique incidence. We also present computational statistics of the method as well as convergence results in terms of the number of layers required for accurate results. Concluding remarks are presented in Sec. IV.

II. PROBLEM FORMULATION

The problem governing the propagation of a polarized plane wave obliquely incident to the surface of a cholesteric liquid crystal cell is formulated in this section. The directors of cholesteric liquid crystals follow a helical structure which is periodic along the normal coordinate (z axis) and has a period P_o, known as the pitch length. For such a material, the corresponding dielectric tensor has the following form:

$$\hat{\epsilon}(z) = \begin{bmatrix} \epsilon_{xx} & \epsilon_{xy} & 0 \\ \epsilon_{yx} & \epsilon_{yy} & 0 \\ 0 & 0 & \epsilon_{zz} \end{bmatrix}, \tag{1}$$

where

$$\begin{aligned} \epsilon_{xx} &= \frac{1}{2}\left(n_e^2 + n_o^2\right) + \frac{1}{2}\left(n_e^2 - n_o^2\right)\cos\left(\frac{4\pi}{P_o}z\right), \\ \epsilon_{yy} &= \frac{1}{2}\left(n_e^2 + n_o^2\right) - \frac{1}{2}\left(n_e^2 - n_o^2\right)\cos\left(\frac{4\pi}{P_o}z\right), \\ \epsilon_{zz} &= n_o^2, \quad \epsilon_{xy} = \epsilon_{yx} = \frac{1}{2}\left(n_e^2 - n_o^2\right)\sin\left(\frac{4\pi}{P_o}z\right). \end{aligned} \tag{2}$$

The refractive indices n_o and n_e correspond to the ordinary and extraordinary waves. In terms of the dielectric constants perpendicular and parallel to the directors of the liquid crystal, these are given by $n_o^2 = \epsilon_\perp$ and $n_e^2 = \epsilon_\parallel$, respectively.

The geometry under investigation is illustrated in Fig. 1. A linearly, circularly, or elliptically polarized plane wave is obliquely incident on the cell. Part of the incident wave energy will be reflected back, whereas the remaining part of the energy will be transmitted through the cell. According to Snell's laws, the reflection (θ_r) and transmission (θ_t) angles are equal to the incident angle (θ_i).

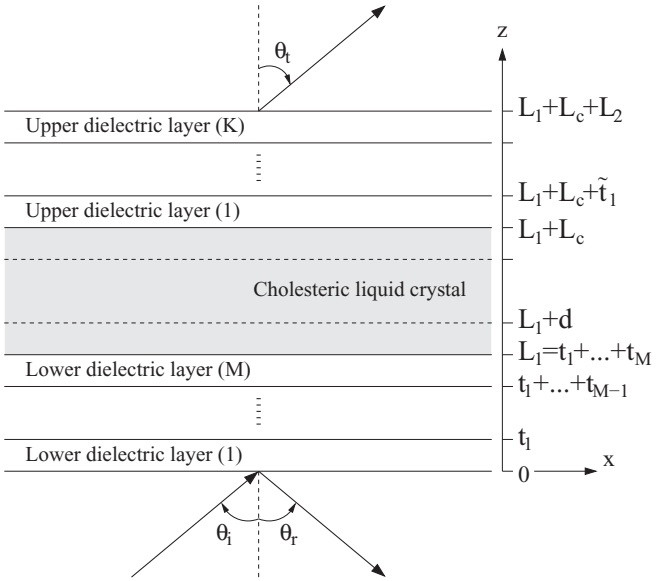

FIG. 1. Geometry of a cholesteric liquid crystal sandwiched between layers of dielectric material.

The formulation of the problem begins with the two time-harmonic curl equations of Maxwell given by

$$\nabla \times \boldsymbol{E} = -j\omega\mu_o \boldsymbol{H}, \tag{3a}$$

$$\nabla \times \boldsymbol{H} = j\omega\epsilon_o \hat{\epsilon}\boldsymbol{E}. \tag{3b}$$

Assuming that the incident plane wave is normal to the y axis, it is evident that

$$\frac{\partial F}{\partial y} = 0, \quad \text{where} \quad F = \{E_x, E_y, E_z, H_x, H_y, H_z\}. \tag{4}$$

In addition, all the scalar field components, in either dielectric or liquid crystal regions, are proportional to $e^{-jk_o n_s (x \sin\theta_i)}$; thus the derivative with respect to x yields

$$\frac{\partial F}{\partial x} = -jk_o S \cdot F, \tag{5}$$

where $S = n_s \sin\theta_i$ and n_s is the refractive index of the exterior region. Substituting Eqs. (4) and (5) in the scalar Maxwell equations derived from Eqs. (3), one can obtain the governing field expressions for either dielectric or liquid crystal regions. These will be derived and presented in the following two subsections.

A. Governing equations for a dielectric region

The cholesteric liquid crystal is sandwiched between layers of dielectrics. Assuming the dielectric constant of one such layer is given by ϵ_d, and using Eqs. (4) and (5) in the two

Maxwell curl equations, we obtain

$$\frac{\partial E_y}{\partial z} = jk_o\eta_o H_x, \tag{6a}$$
$$\frac{\partial E_x}{\partial z} = jk_o\eta_o\left(\frac{S^2}{\epsilon_d} - 1\right)H_y, \tag{6b}$$
$$\frac{\partial H_y}{\partial z} = -j\frac{k_o}{\eta_o}\epsilon_d E_x, \tag{6c}$$
$$\frac{\partial H_x}{\partial z} = j\frac{k_o}{\eta_o}(\epsilon_d - S^2)E_y. \tag{6d}$$

Equations (6a)–(6d) can be written in a more convenient form,

$$\frac{\partial u_1}{\partial z} = jk_o(b_{14}u_4), \tag{7a}$$
$$\frac{\partial u_2}{\partial z} = jk_o(u_3), \tag{7b}$$
$$\frac{\partial u_3}{\partial z} = jk_o(b_{32}u_2), \tag{7c}$$
$$\frac{\partial u_4}{\partial z} = jk_o(b_{41}u_1), \tag{7d}$$

where

$$u_1 = E_x, \quad u_2 = E_y, \quad u_3 = \eta_o H_x, \quad u_4 = \eta_o H_y, \tag{8a}$$
$$b_{14} = S^2/\epsilon_d - 1, \quad b_{41} = -\epsilon_d, \quad b_{32} = \epsilon_d - S^2. \tag{8b}$$

The generic solution of the above system of differential equations has the following form:

$$u \propto e^{-jk_o nz}, \tag{9}$$

where n is the unknown governing refractive index. Consequently, the governing system of Eqs. (7a)–(7d) becomes

$$nu_1 + b_{14}u_4 = 0, \tag{10a}$$
$$nu_2 + u_3 = 0, \tag{10b}$$
$$b_{32}u_2 + nu_3 = 0, \tag{10c}$$
$$b_{41}u_1 + nu_4 = 0. \tag{10d}$$

In matrix form, the above system of equations can be expressed as

$$\begin{bmatrix} n & 0 & 0 & b_{14} \\ b_{41} & 0 & 0 & n \\ 0 & n & 1 & 0 \\ 0 & b_{32} & n & 0 \end{bmatrix} \begin{bmatrix} u_1 \\ u_2 \\ u_3 \\ u_4 \end{bmatrix} = \begin{bmatrix} 0 \\ 0 \\ 0 \\ 0 \end{bmatrix}. \tag{11}$$

For a nontrivial solution, the determinant of the coefficient matrix must be zero. This results in a quartic secular equation with respect to the unknown refractive index; i.e.,

$$(n^2 - b_{32})(n^2 - b_{14}b_{41}) = 0, \tag{12}$$

with solutions

$$n_{1,4} = \pm\sqrt{b_{14}b_{41}}, \quad n_{2,3} = \pm\sqrt{b_{32}}. \tag{13}$$

As seen from the linear system in Eq. (11), the quantities u_1 and u_4 are totally decoupled from the quantities u_3 and u_4. As a result, the governing expressions of u_1 and u_4 can be written as the superposition of the generic form, shown in Eq. (9), for the two values of the refractive indices n_1 and n_4. Similarly, the governing expressions of u_2 and u_3 can be written as the superposition of the same generic form, but instead, using the two refractive indices n_2 and n_3. Consequently, the corresponding expressions for u_i are given by

$$u_1(z) = q_{11}A_D e^{-jk_o n_1 z} + q_{14}D_D e^{-jk_o n_4 z}, \tag{14a}$$
$$u_2(z) = q_{22}B_D e^{-jk_o n_2 z} + q_{23}C_D e^{-jk_o n_3 z}, \tag{14b}$$
$$u_3(z) = q_{32}B_D e^{-jk_o n_2 z} + q_{33}C_D e^{-jk_o n_3 z}, \tag{14c}$$
$$u_4(z) = q_{41}A_D e^{-jk_o n_1 z} + q_{44}D_D e^{-jk_o n_4 z}, \tag{14d}$$

where

$$q_{11} = 1, \quad q_{14} = 1, \quad q_{41} = -\frac{b_{41}}{n_1}, \quad q_{44} = -\frac{b_{41}}{n_4}, \tag{15a}$$
$$q_{22} = 1, \quad q_{23} = 1, \quad q_{32} = -n_2, \quad q_{33} = -n_3. \tag{15b}$$

Subscript D indicates dielectric layer.

B. Governing equations for the liquid crystal

The dielectric tensor of the cholesteric liquid crystal is given by Eqs. (1) and (2). Since the dielectric properties of the medium are dependent on the z coordinate, the liquid crystal is subdivided into electrically thin layers in which the entries of the dielectric tensor are considered constants. Consequently, the analysis in this subsection is valid for a thin layer of liquid crystal where the directors are nematic in nature oriented along the same direction. Thus following the same approach as for the dielectric region presented in the previous subsection, the governing set of differential equations for the cholesteric liquid crystal (anisotropic medium) is given by

$$\frac{\partial E_y}{\partial z} = jk_o\eta_o H_x, \tag{16a}$$
$$\frac{\partial E_x}{\partial z} = jk_o\eta_o\left(\frac{S^2}{\epsilon_{zz}} - 1\right)H_y, \tag{16b}$$
$$\frac{\partial H_y}{\partial z} = -j\frac{k_o}{\eta_o}\{\epsilon_{xx}E_x + \epsilon_{xy}E_y\}, \tag{16c}$$
$$\frac{\partial H_x}{\partial z} = j\frac{k_o}{\eta_o}\{\epsilon_{yx}E_x + (\epsilon_{yy} - S^2)E_y\}. \tag{16d}$$

Introducing the same notation as in Eqs. (7), the above set of equations can be written in a more convenient form given by

$$\frac{\partial u_1}{\partial z} = jk_o(c_{14}u_4), \tag{17a}$$
$$\frac{\partial u_2}{\partial z} = jk_o(u_3), \tag{17b}$$
$$\frac{\partial u_3}{\partial z} = jk_o(c_{31}u_1 + c_{32}u_2), \tag{17c}$$
$$\frac{\partial u_4}{\partial z} = jk_o(c_{41}u_1 + c_{42}u_2), \tag{17d}$$

where

$$u_1 = E_x, \quad u_2 = E_y, \quad u_3 = \eta_o H_x, \quad u_4 = \eta_o H_y, \tag{18a}$$
$$c_{14} = \frac{S^2}{\epsilon_{zz}} - 1, \quad c_{41} = -\epsilon_{xx}, \quad c_{42} = -\epsilon_{xy}, \tag{18b}$$
$$c_{31} = \epsilon_{yx}, \quad c_{32} = \epsilon_{yy} - S^2. \tag{18c}$$

As in the dielectric case, the generic solution of the above system of equations is of the following form:

$$u \propto e^{-jk_o nz}, \tag{19}$$

where n is the unknown governing refractive index. Differentiating with respect to the z coordinate and substituting the result in Eqs. (17) yields the following set of linear equations:

$$nu_1 + c_{14}u_4 = 0, \tag{20a}$$
$$nu_2 + u_3 = 0, \tag{20b}$$
$$c_{31}u_1 + c_{32}u_2 + nu_3 = 0, \tag{20c}$$
$$c_{41}u_1 + c_{42}u_2 + nu_4 = 0. \tag{20d}$$

In matrix form, the above system of equations can be written as

$$\begin{bmatrix} n & 0 & 0 & c_{14} \\ 0 & n & 1 & 0 \\ c_{31} & c_{32} & n & 0 \\ c_{41} & c_{42} & 0 & n \end{bmatrix} \begin{bmatrix} u_1 \\ u_2 \\ u_3 \\ u_4 \end{bmatrix} = \begin{bmatrix} 0 \\ 0 \\ 0 \\ 0 \end{bmatrix}. \tag{21}$$

For a nontrivial solution, the determinant of the coefficient matrix must be zero. This will result in solving a quartic secular equation with respect to the unknown refractive index; i.e.,

$$n^4 - \alpha n^2 + \beta = 0, \tag{22}$$

where $\alpha = c_{32} + c_{14}c_{41}$ and $\beta = c_{14}c_{41}c_{32} - c_{14}c_{41}c_{31}$. The roots of Eq. (22) are

$$n_{1,2,3,4} = \pm\sqrt{\frac{\alpha \pm \sqrt{\alpha^2 - 4\beta}}{2}}. \tag{23}$$

The complete valid solution for u_i, where $i = 1,2,3,4$ is a superposition of the generic form, given in Eq. (19), for the four distinct values of the refractive index obtained in Eq. (23). As a result, the corresponding expressions for u_i are given by

$$u_1(z) = w_{11}Ae^{-jk_o n_1 z} + w_{12}Be^{-jk_o n_2 z} + w_{13}Ce^{-jk_o n_3 z} + w_{14}De^{-jk_o n_4 z}, \tag{24a}$$
$$u_2(z) = w_{21}Ae^{-jk_o n_1 z} + w_{22}Be^{-jk_o n_2 z} + w_{23}Ce^{-jk_o n_3 z} + w_{24}De^{-jk_o n_4 z}, \tag{24b}$$
$$u_3(z) = w_{31}Ae^{-jk_o n_1 z} + w_{32}Be^{-jk_o n_2 z} + w_{33}Ce^{-jk_o n_3 z} + w_{34}De^{-jk_o n_4 z}, \tag{24c}$$
$$u_4(z) = w_{41}Ae^{-jk_o n_1 z} + w_{42}Be^{-jk_o n_2 z} + w_{43}Ce^{-jk_o n_3 z} + w_{44}De^{-jk_o n_4 z}, \tag{24d}$$

where

$$w_{1j} = \frac{n_j^2 - c_{32}}{c_{31}}, \quad j = 1,2,3,4, \tag{25a}$$
$$w_{2j} = 1, \quad j = 1,2,3,4, \tag{25b}$$
$$w_{3j} = -n_j, \quad j = 1,2,3,4, \tag{25c}$$
$$w_{4j} = \frac{n_j\left(c_{32} - n_j^2\right)}{c_{14}c_{31}}, \quad j = 1,2,3,4. \tag{25d}$$

C. Governing field expressions for the exterior region

The exterior region is divided into two subregions: the lower region where the incident and reflected fields exist, and the upper region where the transmitted field exists. The incident plane wave impinges on the liquid crystal cell at an angle θ_i with respect to the normal to the cell, whereas the reflected wave forms an angle $\theta_r = \theta_i$ with respect to the normal. Similarly, the transmitted wave forms an angle $\theta_t = \theta_i$ with respect to the normal. The polarization of the incident wave could be either linear, circular, or even elliptical. The refractive index of the medium in the exterior region is defined as n_s. As a result, the incident fields, for a generic type of polarization, can be written as

$$\boldsymbol{E}^i = \{\hat{a}_y E_{01} + (\hat{a}_z \sin\theta_i - \hat{a}_x \cos\theta_i)E_{02}\} \cdot e^{-jk_o n_s(x\sin\theta_i + z\cos\theta_i)}, \tag{26a}$$
$$\boldsymbol{H}^i = \frac{n_s}{\eta_o}\{(\hat{a}_z \sin\theta_i - \hat{a}_x \cos\theta_i)E_{01} - \hat{a}_y E_{02}\} \cdot e^{-jk_o n_s(x\sin\theta_i + z\cos\theta_i)}. \tag{26b}$$

The polarization of the incident wave can be set by the choice of the amplitudes E_{01} and E_{02}. Specifically, the following combinations can be set:

$E_{01} = 1, \quad E_{02} = 0 \rightarrow$ perpendicular polarization,
$E_{01} = 0, \quad E_{02} = 1 \rightarrow$ parallel polarization,
$E_{01} = 1, \quad E_{02} = +j \rightarrow$ RH circular polarization,
$E_{01} = 1, \quad E_{02} = -j \rightarrow$ LH circular polarization,
$E_{01} = 1, \quad E_{02} = +\nu j \rightarrow$ RH elliptical polarization,
$E_{01} = 1, \quad E_{02} = -\nu j \rightarrow$ LH elliptical polarization,

where $\nu \neq 1$, RH stands for right hand, and LH stands for left hand. The corresponding reflected field expressions can be written as

$$\boldsymbol{E}^r = \{\hat{a}_y \Gamma_\perp + (\hat{a}_x \cos\theta_i + \hat{a}_z \sin\theta_i)\Gamma_\parallel\} \cdot e^{-jk_o n_s(x\sin\theta_i - z\cos\theta_i)}, \tag{27a}$$
$$\boldsymbol{H}^r = \frac{n_s}{\eta_o}\{(\hat{a}_x \cos\theta_i + \hat{a}_z \sin\theta_i)\Gamma_\perp - \hat{a}_y \Gamma_\parallel\} \cdot e^{-jk_o n_s(x\sin\theta_i - z\cos\theta_i)}, \tag{27b}$$

where $\Gamma_\perp$ and $\Gamma_\parallel$ correspond to the reflection coefficients perpendicular and parallel to the plane of incidence, respectively. Likewise, the corresponding expressions for the transmitted fields in the upper region are given by

$$\boldsymbol{E}^t = \{\hat{a}_y T_\perp + (\hat{a}_z \sin\theta_i - \hat{a}_x \cos\theta_i)T_\parallel\} \cdot e^{-jk_o n_s(x\sin\theta_i + z\cos\theta_i)}, \tag{28a}$$
$$\boldsymbol{H}^t = \frac{n_s}{\eta_o}\{(\hat{a}_z \sin\theta_i - \hat{a}_x \cos\theta_i)T_\perp - \hat{a}_y T_\parallel\} \cdot e^{-jk_o n_s(x\sin\theta_i + z\cos\theta_i)}, \tag{28b}$$

where $T_\perp$ and $T_\parallel$ correspond to the transmission coefficients perpendicular and parallel to the plane of incidence, respectively.

Now, based on the definition of the incident, reflected, and transmitted fields in the lower and upper exterior regions, the corresponding expressions for u_j's can be written in a more convenient form. Specifically, for the lower exterior region,

we have

$$u_1(z) = \cos\theta_i \left(\Gamma_\parallel e^{jk_o n_s z\cos\theta_i} - E_{02} e^{-jk_o n_s z\cos\theta_i}\right), \quad (29a)$$

$$u_2(z) = \Gamma_\perp e^{jk_o n_s z\cos\theta_i} + E_{01} e^{-jk_o n_s z\cos\theta_i}, \quad (29b)$$

$$u_3(z) = n_s\cos\theta_i \left(\Gamma_\perp e^{jk_o n_s z\cos\theta_i} - E_{01} e^{-jk_o n_s z\cos\theta_i}\right), \quad (29c)$$

$$u_4(z) = -n_s \left(\Gamma_\parallel e^{jk_o n_s z\cos\theta_i} + E_{02} e^{-jk_o n_s z\cos\theta_i}\right). \quad (29d)$$

Similarly, for the upper exterior region, the z-dependent expressions for the u_j's are given by

$$u_1(z) = -\cos\theta_i T_\parallel e^{-jk_o n_s z\cos\theta_i}, \quad (30a)$$

$$u_2(z) = T_\perp e^{-jk_o n_s z\cos\theta_i}, \quad (30b)$$

$$u_3(z) = -n_s\cos\theta_i T_\perp e^{-jk_o n_s z\cos\theta_i}, \quad (30c)$$

$$u_4(z) = -n_s T_\parallel e^{-jk_o n_s z\cos\theta_i}. \quad (30d)$$

D. Mode-matching approach

Once we have defined the governing fields in the exterior region, the dielectric layers, and the cholesteric liquid crystal, the unknown coefficients can be obtained by enforcing the continuity of the tangential fields at the interfaces. An interface exists between the exterior region and the neighboring dielectric layer (see Fig. 1), between subsequent dielectric layers, between the last dielectric layer and the liquid crystal, etc. In addition, as mentioned previously, the cholesteric liquid crystal was subdivided into N thin homogeneous layers in which the dielectric tensor entries are considered constants. Consequently, the continuity of the tangential fields at those interfaces should be enforced. For each crystal or dielectric layer, there are four unknown coefficients namely A, B, C, and D. For the lower and upper exterior regions, there are two unknown reflection coefficients and two unknown transmission coefficients. Thus the total number of problem unknowns is $4(N + M + K + 1)$, where M and K correspond to the number of dielectric layers below and above the liquid crystal, respectively. Note that enforcement of the tangential electric and magnetic fields is equivalent to the enforcement of u_j, where $j = 1,2,3,4$.

Before imposing the continuity of u_j's at the interfaces, it is important to introduce a transformation on the z coordinate in order to simplify the implementation of the mode-matching approach. In particular, we transform z to $z - z_o$, where z_o is the z coordinate of the lower interface of a given layer. The implementation of the mode-matching approach is demonstrated below by presenting a set of equations obtained after imposing the continuity of u_j's at selected interfaces:

At $z = 0$,

$$\cos\theta_i(\Gamma_\parallel - E_{02}) = q^1_{11}A^1_D + q^1_{14}D^1_D, \quad (31a)$$

$$\Gamma_\perp + E_{01} = q^1_{22}B^1_D + q^1_{23}C^1_D, \quad (31b)$$

$$n_s\cos\theta_i(\Gamma_\perp - E_{01}) = q^1_{32}B^1_D + q^1_{33}C^1_D, \quad (31c)$$

$$-n_s(\Gamma_\parallel + E_{02}) = q^1_{41}A^1_D + q^1_{44}D^1_D. \quad (31d)$$

The superscript on the coefficients q, A, B, C, and D corresponds to the index of the particular dielectric layer.

At $z = L_1$,

$$q^M_{11}A^M_D e^{-jk_o n_1 t_M} + q^M_{14}D^M_D e^{-jk_o n_4 t_M} = w^1_{11}A^1 + w^1_{12}B^1 + w^1_{13}C^1 + w^1_{14}D^1, \quad (32a)$$

$$q^M_{22}B^M_D e^{-jk_o n_2 t_M} + q^M_{23}C^M_D e^{-jk_o n_3 t_M} = w^1_{21}A^1 + w^1_{22}B^1 + w^1_{23}C^1 + w^1_{24}D^1, \quad (32b)$$

$$q^M_{32}B^M_D e^{-jk_o n_2 t_M} + q^M_{33}C^M_D e^{-jk_o n_3 t_M} = w^1_{31}A^1 + w^1_{32}B^1 + w^1_{33}C^1 + w^1_{34}D^1, \quad (32c)$$

$$q^M_{41}A^M_D e^{-jk_o n_1 t_M} + q^M_{44}D^M_D e^{-jk_o n_4 t_M} = w^1_{41}A^1 + w^1_{42}B^1 + w^1_{43}C^1 + w^1_{44}D^1. \quad (32d)$$

The superscript on the constants w, A, B, C, and D indicate the layer number within the liquid crystal with thickness $d = L_c/N$.

At $z = L_1 + L_c$,

$$w^N_{11}A^N e^{-jk_o n_1 d} + w^N_{12}B^N e^{-jk_o n_2 d} + w^N_{13}C^N e^{-jk_o n_3 d} + w^N_{14}D^N e^{-jk_o n_4 d} = q^1_{11}\widetilde{A}^1_D + q^1_{14}\widetilde{D}^1_D, \quad (33a)$$

$$w^N_{21}A^N e^{-jk_o n_1 d} + w^N_{22}B^N e^{-jk_o n_2 d} + w^N_{23}C^N e^{-jk_o n_3 d} + w^N_{24}D^N e^{-jk_o n_4 d} = q^1_{22}\widetilde{B}^1_D + q^1_{23}\widetilde{C}^1_D, \quad (33b)$$

$$w^N_{31}A^N e^{-jk_o n_1 d} + w^N_{32}B^N e^{-jk_o n_2 d} + w^N_{33}C^N e^{-jk_o n_3 d} + w^N_{34}D^N e^{-jk_o n_4 d} = q^1_{32}\widetilde{B}^1_D + q^1_{33}\widetilde{C}^1_D, \quad (33c)$$

$$w^N_{41}A^N e^{-jk_o n_1 d} + w^N_{42}B^N e^{-jk_o n_2 d} + w^N_{43}C^N e^{-jk_o n_3 d} + w^N_{44}D^N e^{-jk_o n_4 d} = q^1_{41}\widetilde{A}^1_D + q^1_{44}\widetilde{D}^1_D. \quad (33d)$$

The constants $\widetilde{A}_D, \widetilde{B}_D, \widetilde{C}_D$, and $\widetilde{D}_D$ correspond to the dielectric layers of the upper cell; the superscript represents the dielectric layer number.

At $z = L_1 + L_c + L_2$,

$$q^K_{11}\widetilde{A}^K_D e^{-jk_o n_1 \widetilde{t}_K} + q^K_{14}\widetilde{D}^K_D e^{-jk_o n_4 \widetilde{t}_K} = -T_\parallel\cos\theta_i, \quad (34a)$$

$$q^K_{22}\widetilde{B}^K_D e^{-jk_o n_2 \widetilde{t}_K} + q^K_{23}\widetilde{C}^K_D e^{-jk_o n_3 \widetilde{t}_K} = T_\perp, \quad (34b)$$

$$q^K_{32}\widetilde{B}^K_D e^{-jk_o n_2 \widetilde{t}_K} + q^K_{33}\widetilde{C}^K_D e^{-jk_o n_3 \widetilde{t}_K} = -n_s\cos\theta_i T_\perp, \quad (34c)$$

$$q^K_{41}\widetilde{A}^K_D e^{-jk_o n_1 \widetilde{t}_K} + q^K_{44}\widetilde{D}^K_D e^{-jk_o n_4 \widetilde{t}_K} = -n_s T_\parallel. \quad (34d)$$

The above equations can be expressed in matrix form with the unknown vector consisting of the expansion coefficients, the two reflection coefficients, and the two transmission coefficients. Solving this matrix system, the unknown vector can be obtained for a given incident angle and a given polarization. Once the reflection and transmission coefficients are obtained, the reflectance and transmittance can be computed using

$$\gamma = \frac{|\Gamma_\parallel|^2 + |\Gamma_\perp|^2}{|E_{01}|^2 + |E_{02}|^2}, \quad (35)$$

$$\tau = \frac{|T_\parallel|^2 + |T_\perp|^2}{|E_{01}|^2 + |E_{02}|^2}. \quad (36)$$

III. NUMERICAL RESULTS

The eigenmode analysis and mode-matching approach presented in the previous section were verified against published data found in the literature. We considered the same exact cases investigated by Yang *et al.* [36] in order to provide comparisons to our simulations. In their paper, they used the Jones matrix method to develop an improved numerical method where multiple reflections were taken into account. However, their approach is only suitable for normal incidence and in the absence of dielectric layers external to the liquid

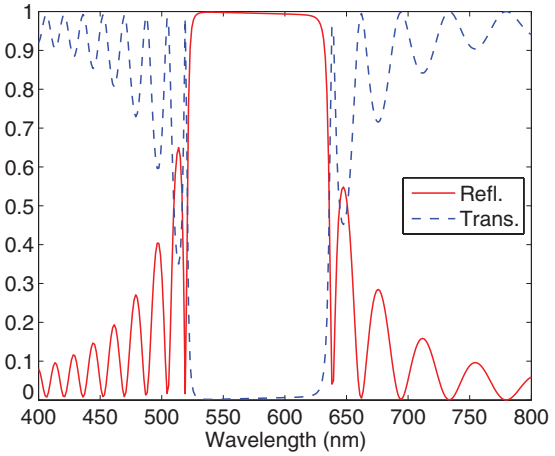

FIG. 2. (Color online) Reflectance and transmittance of a cholesteric liquid crystal for a RH circularly polarized wave at normal incidence.

crystal cell. Their numerical results compared well with those obtained using the Berreman method with some instabilities when the thickness of the cell exceeded $100P_o$. Specifically, we considered a cholesteric liquid crystal with pitch length $P_o = 350$ nm, $n_o = 1.5$, $n_e = 1.8$, $L_c = 10P_o$. The exterior region to the liquid crystal cell is characterized by an isotropic medium of refractive index equal to that of glass; thus there is no reflection from the first interface between the exterior region and the liquid crystal. The incident plane wave is normal to the cell and the polarization is either right-hand circular polarization (RHCP), perpendicular polarization, or parallel polarization. Both the reflectance and transmittance are computed in the entire visible spectrum by considering the reflection and transmission coefficients in both principal planes. Our simulated results are shown in Fig. 2, for the RH circular polarization, in Fig. 3, for perpendicular polarization, and in Fig. 4, for parallel polarization. Comparing with the corresponding figures in Ref. [36], there is an excellent agreement between the improved Jones matrix method and our proposed mode-matching technique.

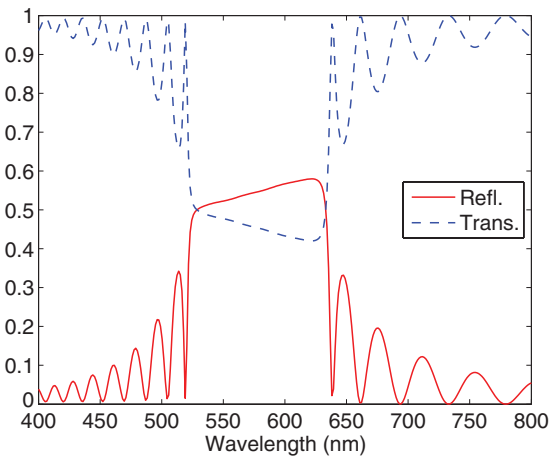

FIG. 3. (Color online) Reflectance and transmittance of a cholesteric liquid crystal for a plane wave polarized perpendicularly to the plane of incidence and at normal incidence.

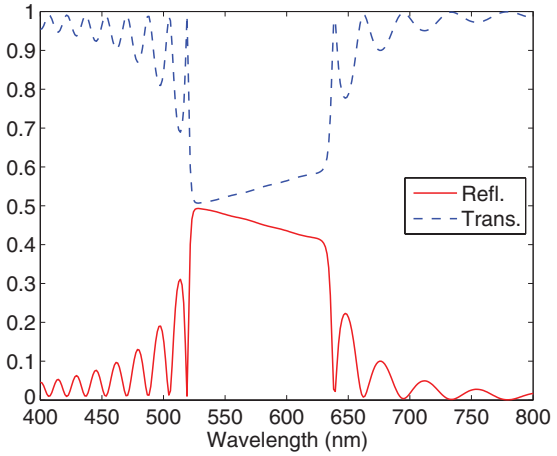

FIG. 4. (Color online) Reflectance and transmittance of a cholesteric liquid crystal for a plane wave polarized parallel to the plane of incidence and at normal incidence.

The advantage of our method, as compared to the improved Jones matrix method presented in Ref. [36], is the ability to obtain reflection and transmission spectra at oblique incidence. Figure 5 illustrates the reflectance of a cholesteric liquid crystal, having the same specifications as above, for a right-hand circularly polarized plane wave at normal and oblique incidence ($\theta_i = 30^\circ$). At oblique incidence, the reflection spectra exhibit the well-known blueshift of the Bragg reflection.

The reflectance as a function of the cell thickness is illustrated in Fig. 6. Our simulation results compare favorably with the corresponding graph depicted in Ref. [36]. As seen from this figure, the Bragg reflection is established only when the thickness of the cholesteric liquid crystal cell is approximately ten times the pitch length of the helical molecular structure.

Our proposed method is also generic in terms of adding as many dielectric layers as needed in the exterior region. The versatility of the method is illustrated by examining the same geometry investigated by Xu *et al.* [37]. Specifically, they considered a cholesteric liquid crystal cell of thickness $L_c = 15P_o$, where $P_o = 338$ nm, $n_o = 1.494$, and $n_e = 1.616$. The cell is sandwiched between three dielectric layers at the top and bottom of the cell. The outer layer is glass with a refractive

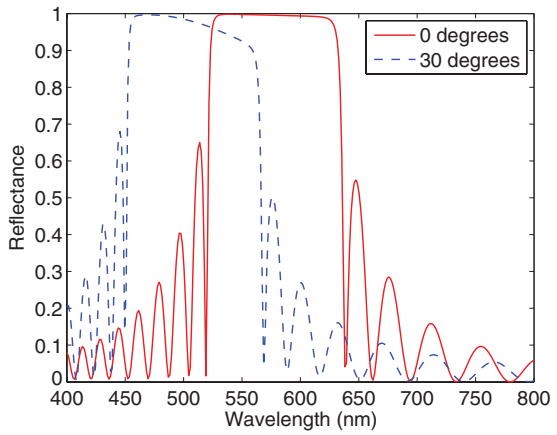

FIG. 5. (Color online) Reflectance of a cholesteric liquid crystal for a RH circularly polarized wave at normal and oblique incidence.

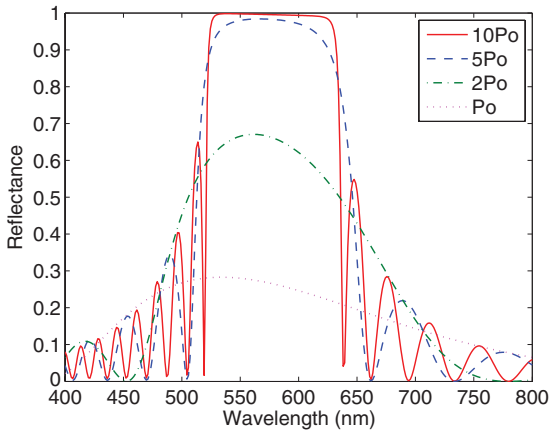

FIG. 6. (Color online) Reflectance of a cholesteric liquid crystal for a RH circularly polarized wave at normal incidence for different cell thicknesses.

index of $n = 1.5$ and thickness of $t = 1.06$ mm. The middle layer is ITO whose refractive index is a function of wavelength [37] and is given by $n(\lambda) = 2.525 - 0.001\,271\lambda$, where λ is given in nanometers (nm). The thickness of ITO is $t = 25$ nm. The inner dielectric layer is a Polyimide alignment layer with refractive index $n = 1.7$ and a thickness of $t = 98$ nm. The corresponding reflectance spectra for normal incidence and oblique incidence at $\theta_i = 30^\circ$ is shown in Fig. 7 for a right-handed circularly polarized incident plane wave. In this case, the medium of the exterior region is characterized by a refractive index of $n = 1.5$ thus there is no reflection from the first dielectric interface, i.e., between the exterior region and the glass layer. However, if the exterior region is taken to be air, it is evident from Fig. 8 that there is significant reflection from the first air-glass interface. This can be alleviated by properly designing an antireflective layer for the visible spectrum to be placed at the first air-glass interface.

The accuracy of the proposed numerical approach was evaluated in terms of the number of layers considered in the cholesteric liquid crystal. Note that the dielectric layers (e.g. glass, ITO, polyimide) are not subdivided into smaller layers.

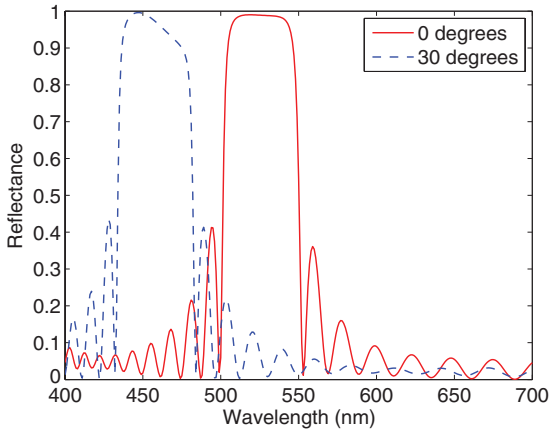

FIG. 7. (Color online) Reflectance of a cholesteric liquid crystal sandwiched between layers of glass, ITO, and polyimide for a RH circularly polarized wave; the medium of the exterior region has the same refractive index as that of glass.

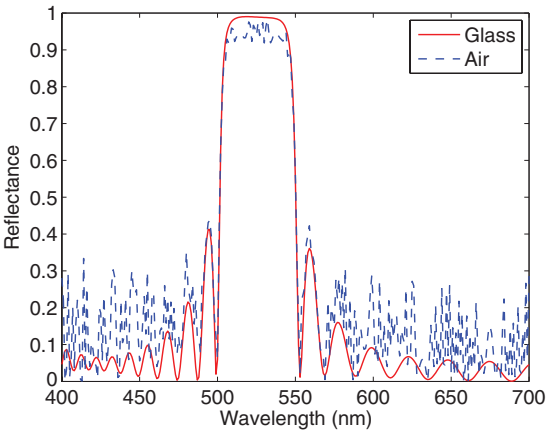

FIG. 8. (Color online) Reflectance of a cholesteric liquid crystal sandwiched between layers of glass, ITO, and polyimide for a RH circularly polarized wave; a comparison between two cases of exterior region: air and glass.

The only approximation introduced in the proposed method is the staircasing of the dielectric tensor profile along the helical axis. For this reason, we are plotting the reflectance at $\lambda = 550$ nm, for normal and oblique incidence, as a function of the number of layers per pitch inside the cholesteric liquid crystal. The incident plane wave was right-hand circularly polarized. The corresponding graph is shown in Fig. 9. It can be seen that approximately 10 layers per pitch is sufficient to obtain accurate results for the case of normal incidence, whereas for the case of oblique incidence, approximately 20 layers per pitch are required. In terms of solution time on a personal desktop computer, we plotted the CPU time in seconds for a single evaluation point as a function of the number of layers per pitch. The corresponding graph is shown in Fig. 10. As seen, the solution time increases in a nonlinear fashion as the number of layers per pitch increase. When using 20 layers per pitch, which is sufficient to provide accurate results at oblique angles of incidence, the required solution time per evaluation point is 0.5 sec; for 30 layers per pitch, the corresponding solution time increases to 1.7 sec per evaluation point. Based on our experience, there is no need to subdivide the liquid crystal into more than 30 layers per pitch.

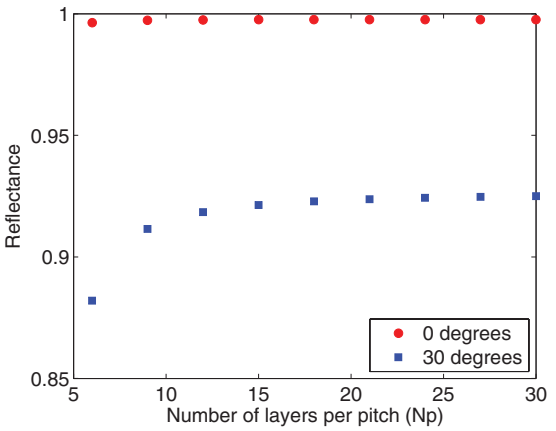

FIG. 9. (Color online) Convergence of the reflectance as a function of the number of subdivisions per pitch length.

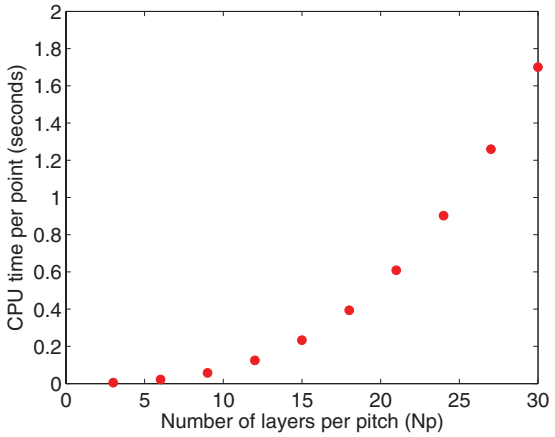

FIG. 10. (Color online) CPU solution time (in seconds) per point as a function of the number of subdivisions per pitch length.

IV. CONCLUSIONS

In this paper, we developed an exact formulation based on an eigenvalue analysis and a mode-matching technique imposed at the interfaces between stratified media. The eigenvalue analysis was applied on isotropic dielectric layers as well as on anisotropic cholesteric liquid crystals exhibiting a right-handed twist of the director field. The eigenvalue analysis provided governing solutions for the fields inside the media as well as the supported propagation characteristics along the helical axis. A linearly, circularly, or elliptically polarized incident plane wave was considered at oblique angles. The formulation presented in Sec. II is exact and introduces no approximations. The only compromise made was the staircasing of the helical profile of the dielectric tensor along the helical axis. In other words, the cholesteric liquid crystal was subdivided into N layers assuming a homogeneous nematic orientation of the director fields, thus the tensor entries were considered constant within each of these layers. As a result of this approach, a matrix system of linear equations was obtained, which was solved in order to obtain the corresponding reflection and transmission coefficients on the two principal planes. The obtained numerical results verify the accuracy and the effectiveness of the proposed method in dealing with this type of liquid crystal problems.

[1] P. de Gennes and J. Prost, *The Physics of Liquid Crystals*, 2nd ed. (Clarendon Press, Oxford, 1995).
[2] D. K. Yang and S. T. Wu, *Fundamentals of Liquid Crystal Devices* (John Wiley & Sons, Chichester, West Sussex, UK, 2006).
[3] R. C. Jones, J. Opt. Soc. Am. **31**, 488 (1941).
[4] D. W. Berreman and T. J. Scheffer, Mol. Cryst. Liq. Cryst. **11**, 395 (1970).
[5] D. W. Berreman, J. Opt. Soc. Am. **62**, 502 (1971).
[6] C. Gu and P. Yeh, J. Opt. Soc. Am. A **10**, 966 (1993).
[7] A. Lien, Appl. Phys. Lett. **57**, 2767 (1990).
[8] A. Lien, J. Appl. Phys. **67**, 2853 (1990).
[9] P. Yeh, J. Opt. Soc. Am. **72**, 507 (1982).
[10] H. L. Ong, Appl. Phys. Lett. **59**, 155 (1991).
[11] H. Wohler and M. E. Becker, Optoelectron. Rev. **10**, 23 (2002).
[12] D. W. Berreman, J. Opt. Soc. Am. **63**, 1374 (1973).
[13] H. Wohler, G. Haas, M. Fritsch, and D. A. Mlynski, J. Opt. Soc. Am. A **5**, 1554 (1988).
[14] K. Lu and B. E. A. Saleh, Opt. Lett. **17**, 1557 (1992).
[15] Q. Hong, T. X. Wu, and S. T. Wu, Liq. Cryst. **30**, 367 (2003).
[16] H. L. Ong, J. Opt. Soc. Am. A **8**, 303 (1991).
[17] K. Eidner, G. Mayer, M. Schmidt, and H. Schmiedel, Mol. Cryst. Liq. Cryst. **172**, 191 (1989).
[18] A. Lakhtakia, Optik **119**, 253 (2008).
[19] J. A. Reyes and A. Lakhtakia, Opt. Commun. **266**, 565 (2006).
[20] A. Lakhtakia and R. Messier, *Sculptured Thin Films: Nanoengineered Morphology and Optics* (SPIE, Bellingham, WA, 2005).
[21] C. W. Oseen, J. Chem. Soc. Faraday Trans. II **29**, 883 (1933).
[22] A. Lakhtakia, Opt. Commun. **261**, 213 (2006).
[23] C. W. Oseen, Ark. Mat. Astron. Fys. A **21**, 14 (1925).
[24] H. de Vries, Acta Crystallogr. **4**, 219 (1951).
[25] W. Cao, Ph.D. thesis, Kent State University, 2005.
[26] E. Miraldi, C. Oldano, P. I. Taverna, and L. Trossi, Mol. Cryst. Liq. Cryst. **103**, 155 (1983).
[27] C. Oldano, E. Miraldi, and P. T. Valabrega, Phys. Rev. A **27**, 3291 (1983).
[28] C. Oldano, Phys. Rev. A **31**, 1014 (1985).
[29] D. O. Smith, Opt. Acta **12**, 13 (1965).
[30] D. O. Smith, Opt. Acta **12**, 193 (1965).
[31] S. Teitler and B. W. Henvis, J. Opt. Soc. Am. **60**, 830 (1970).
[32] E. Reusch, Ann. Phys. Chem. Lpz. **138**, 628 (1869).
[33] I. J. Hodgkinson, A. Lakhtakia, Q. H. Wu, L. D. Silva, and M. W. McCall, Opt. Commun. **239**, 353 (2004).
[34] D. W. Berreman and T. J. Scheffer, Phys. Rev. A **5**, 1397 (1972).
[35] H. Takezoe, K. Hashimoto, Y. Ouchi, M. Hara, A. Fukuda, and E. Kuze, Mol. Cryst. Liq. Cryst. **101**, 329 (1983).
[36] D. K. Yang and X. D. Mi, J. Phys. D **33**, 672 (2000).
[37] M. Xu, F. Xu, and D. K. Yang, J. Appl. Phys. **83**, 1938 (1998).